DRAFT VERSION FEBRUARY 5, 2008
Preprint typeset using LaTeX style emulateapj v. 6/22/04

DIFFUSE LIGHT IN THE VIRGO CLUSTER

J. CHRISTOPHER MIHOS, PAUL HARDING, JOHN FELDMEIER[1], AND HEATHER MORRISON
Department of Astronomy, Case Western Reserve University, 10900 Euclid Ave, Cleveland, OH 44106
Draft version February 5, 2008

ABSTRACT

We present deep optical imaging of the inner $\sim 1.5^\circ$x1.5° of the Virgo cluster to search for diffuse intracluster light (ICL). Our image reaches a 1σ depth of μ_V=28.5 mag/arcsec^2 — 1.5 mag/arcsec^2 deeper than previous surveys — and reveals an intricate web of diffuse intracluster light. We see several long (>100 kpc) tidal streamers, as well as a myriad of smaller-scale tidal tails and bridges between galaxies. The diffuse halo of M87 is traced out to nearly 200 kpc, appearing very irregular on these scales, while significant diffuse light is also detected around the M84/M86 pair. Several galaxies in the core are embedded in common envelopes, suggesting they are true physical subgroups. The complex substructure of Virgo's diffuse ICL reflects the hierarchical nature of cluster assembly, rather than being the product of smooth accretion around a central galaxy.

Subject headings: galaxies: clusters: individual (Virgo) — galaxies: interactions

1. INTRODUCTION

The diffuse intracluster light (ICL) in galaxy clusters is a valuable tool for studying their dynamical history. First identified (see Vílchez-Gómez 1999 for review) and quantified (e.g., Uson, Boughn, & Kuhn 1991; Bernstein et al. 1995; Feldmeier et al. 2002, 2004) using deep broadband imaging, the ICL has also been detected both in individual stars (Ferguson, Tanvir, & von Hippel 1998; Durrell et al. 2002) and intracluster planetary nebulae (IPNe; see Feldmeier et al. 2004 and Aguerri et al. 2005 and references therein), the latter opening up a new field studying ICL kinematics (Arnaboldi et al. 2004; Gerhard et al. 2005). On the theoretical front, N-body simulations of galaxy clusters are now starting to yield high-resolution predictions of the spatial and kinematic distribution of ICL (e.g., Willman et al. 2004; Murante et al. 2004; Sommer-Larsen, Romeo, & Portinari 2005), and showing that the formation of the ICL is intimately linked to tidal stripping during the hierarchical assembly of clusters. The phase-space distribution of the ICL thus holds important information about the detailed dynamical state and assembly history of a galaxy cluster.

In this context, the Virgo cluster (at an adopted distance of 16 Mpc) is of particular interest as it shows many signs of being a dynamically complex environment, ideal for the production of ICL. The cluster possesses both spatial (Bingelli, Sandage, & Tammann 1987) and kinematic (Bingelli, Popescu, & Tammann 1993) substructure, with different subgroups possessing different morphological mixes of galaxies (Bingelli et al. 1987). Many of the cluster galaxies are kinematically disturbed (Rubin, Waterman, & Kenney 1999), indicative of strong, ongoing tidal interactions. Deep photographic imaging (e.g., Malin 1994; Katsiyannis et al. 1998) also show tidal features around many Virgo galaxies, as well as an extended stellar envelope around M87 (Weil, Bland-Hawthorn, & Malin 1997). Studies of the ICL in Virgo also hint at an irregular structure: the distribution of intracluster PNe show marked field-to-field variations (Durrell et al. 2002; Feldmeier et al. 2004; Aguerri et al. 2005), suggestive of a poorly mixed ICL.

However, quantifying the large-scale structure of the ICL in nearby clusters like Virgo has actually proved quite difficult. The relatively small field of view of most telescope/CCD systems makes it hard to survey nearby clusters of large angular size. Deep surface photometry also is hindered by the need to accurately flat field over degree scales, while IPNe surveys to date have not gone deep enough to uniformly sample the full line-of-sight depth of the Virgo cluster. Accordingly, the distribution of ICL in Virgo is still poorly determined, yet it is here that there is a wealth of high spatial resolution ancillary data on the properties of the galaxies and hot intracluster medium.

To address this disparity and make *quantitative, large-scale measurements* of the diffuse light in Virgo, we have begun a deep imaging study of Virgo's core using Case's Burrell Schmidt telescope. Because the Schmidt's wide field of view is imaged onto a single CCD chip, highly accurate flat fielding is possible. Its closed-tube design and extensive optical baffling significantly reduce scattered light problems compared to open-tube telescopes. As such, the Burrell Schmidt is optimally suited for deep, wide-field surface photometry. Here we report on the first season of observations which have revealed Virgo's intricate web of diffuse ICL.

2. IMAGING TECHNIQUE

Deep images of the Virgo cluster were taken during photometric nights in March and April 2004 using the recently refurbished 0.6m Burrell Schmidt telescope (for technical details of the refurbishment see Harding et al. 2005 in preparation, and Feldmeier et al. 2002 for details of the observing and data reduction strategies). The field of view of the Schmidt and its SITe 2048x4096 CCD is approximately 1.5°x0.75°, with $1.45''$ pixels and the long axis of the chip oriented east-west. A total of 72 object images were taken, covering the inner 2.25 square degrees of Virgo. Individual images were flattened using a night sky flat built from 127 offset sky pointings bracketing the object exposures in time and position. The object images and blank skies are all 900s exposures taken in Washington M and transformed into Johnson V magnitudes.

Sky subtraction is a challenge when mosaicking together many images which subtend only a portion of the cluster itself. To remove stars and galaxies from the individual images,

Electronic address: mihos@case.edu, harding@dropbear.case.edu, johnf@noao.edu, heather@vegemite.case.edu
[1] NSF Astronomy and Astrophysics Fellow, NOAO Tucson

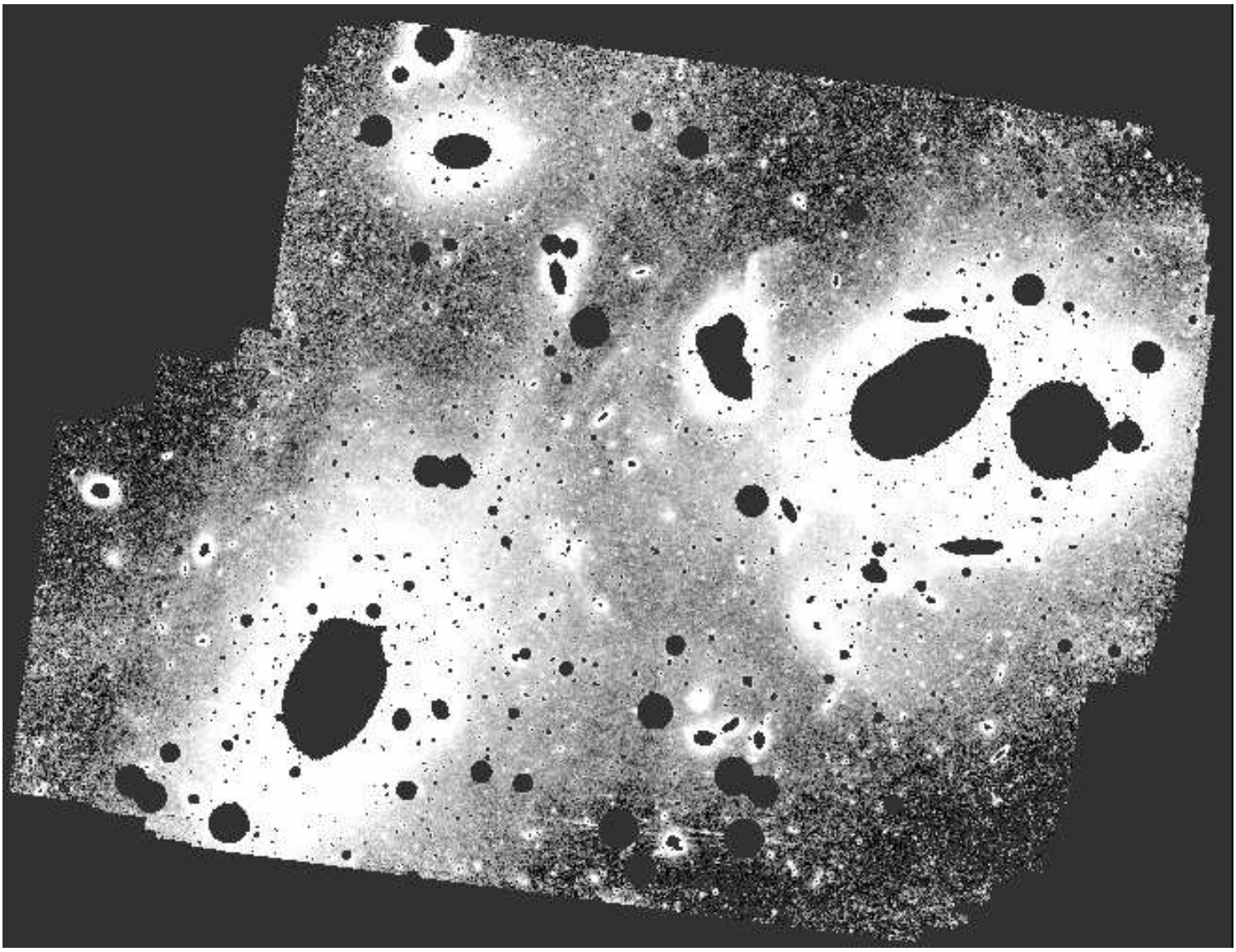

FIG. 1.— Diffuse light in the Virgo cluster core. North is up; east is to the left. The white levels saturate at $\mu_V \sim 26.5$, while the faintest features visible have a surface brightness of $\mu_V \sim 28.5$.

we first mask stars out to where the PSF falls below 3 ADU (μ_V=28), then subtract their extended wings out to 0.5 ADU (μ_V=30). IRAF's OBJMASK task is then used to mask out all extended sources 2.5σ above sky, which essentially removes all bright galaxies. We then remove sky in a multi-step process. We first rebin the masked images into smaller images by calculating the mode in 32x32 pixel bins, and then identify regions on the images which are located far away from any bright galaxy and considered "pure sky"; on average, about 5% of each image is covered by pure sky. Then for each image, we calculate a DC sky level from the mode of the counts in these regions and subtract it from the image. This sky level ranges from 1100–1500 ADU (μ_V=21.6–21.3), depending on a variety of factors such as hour angle, airmass, time of night, and air glow variability. Next, we perform an iterative plane-fitting process where the pure sky regions are used to simultaneously fit individual residual sky planes to each binned image, constrained to minimize frame-to-frame deviations in the pure-sky regions of the final sky-subtracted images. The edge-to-edge gradient of the final fitted sky planes is typically 5 ADU, or $\sim$ 0.35% of the DC sky level.[2]

After sky subtraction of the individual images, the images are registered and medianed together to form the final mosaic. At this point one last plane is also fit and subtracted from the mosaic using the pure sky regions; the edge-to-edge gradient of this final plane is 2 ADU ($\sim$ 0.1% of sky). We then improve the signal-to-noise by medianing the mosaic in a 9x9 pixel boxes ($\sim$ 1 kpc^2), which brings out the faintest features. In the raw image, the 1σ level in the sky is 4.5 ADU (μ_V=27.5), while in the binned, medianed image 1σ=1.7 ADU (μ_V=28.6). This limiting surface brightness is approximately 1.5 mag/arcsec^2 deeper than the deep photographic imaging of Malin (1994).

As a final note, one possible source of confusion in our study is contamination due to the presence of any galactic cirrus in the field, which will be visible as large-scale diffuse

[2] It is important to recognize that fitting and subtracting sky planes can impose a systematic underestimate of the Virgo ICL, since any degree-scale diffuse ICL component will also be subtracted at this step.

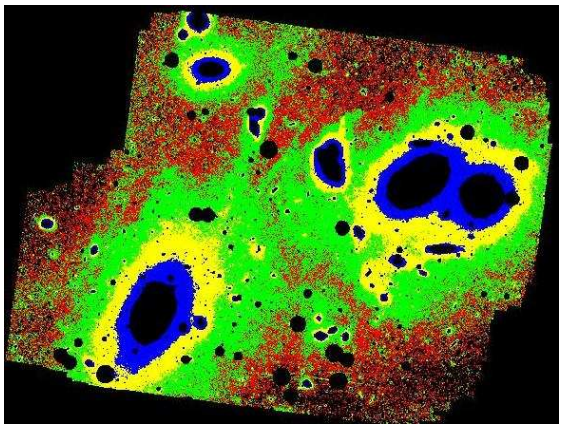

FIG. 2.— Diffuse light in the Virgo cluster, color coded by surface brightness: Blue: μ_V=25-26; Yellow: μ_V=26-27; Green: μ_V=27-28; Red: μ_V=28-29. North is up; east is to the left.

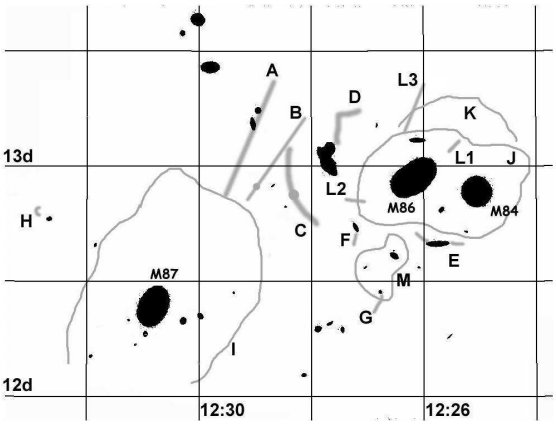

FIG. 3.— Schematic diagram showing location of diffuse features discussed in the text.

reflected light. Examining the IRAS 100μm maps of Virgo, it is clear that a ring of cirrus ($\sim 1.5^\circ$ in diameter) surrounds the Virgo core and may contaminate fields to the southwest and north of our field. Fortuitously, however, the Virgo core itself is quite clear of galactic cirrus, arguing that features we detect are bona fide structures in Virgo's diffuse light.

3. DIFFUSE LIGHT IN VIRGO'S CORE

A greyscale representation of the final binned mosaic is shown in Figure 1, while Figure 2 shows the image colored according to surface brightness. The faintest features visible are at $\mu_V\sim$ 28.5 or about 0.1% of sky. A wealth of diffuse features can be seen in Virgo's ICL, ranging from extended low surface brightness envelopes to long, thin streamers, as well as smaller-scale tidal features associated with many of the Virgo galaxies. Our goal here is to focus on the qualitative morphology of the ICL; a more detailed quantitative analysis will be addressed in later papers. Figure 3 shows a finding chart for the features described below.

In the image, two long streamers can be seen extending to the northwest from M87 at the lower left. One streamer (A) projects through the pair of galaxies NGC 4458/61 and extends beyond, toward a group of galaxies to the north. There is a surface brightness gradient along its length; near M87 it has a surface brightness of μ_V=27, dropping to μ_V=27.8 near the pair. From the point at which it emerges from M87's stellar halo to where it fades into the background, the streamer has total length of 38′ (178 kpc) a characteristic width of 3.′5 (16 kpc), and a total luminosity of $\sim 10^9$ L$_\odot$. Because NGC 4458 and NGC 4461 have a very high velocity relative to one another (Δv = 1296 km/s) it is unlikely the streamer comes from any strong interaction between the pair; instead, stripping from one of the galaxies individually is more likely.

The second streamer (B) is perhaps even more remarkable. Also appearing to emanate from M87 to the northwest, it measures approximately 28′ (130 kpc) long and only 1.2′ (6 kpc) wide, with a peak surface brightness of μ_V=27.0. The low surface brightness dwarf VCC 1149 is projected along the stream, just before the position at which the stream blends into M87's halo; we may well be seeing the destruction of this dwarf in the tidal field of the cluster — a process which may contribute to the variation in the faint end slope of the luminosity function in clusters. The thinness of the stream supports this conjecture, as the low velocity dispersion of dwarf galaxies ensures that stripped tidal streams will be dynamically cold, and not diffuse significantly in the tangential direction. The thinness and linearity of the streamer also argue that the dwarf must be on a highly radial orbit, or one that is seen projected along its orbital plane.

Not all detected streams are linear, however. A broad, curved stream (C) can be seen surrounding a low surface brightness dwarf; the curvature of this stream, arcing away from M87, suggests that the galaxy is orbiting within or around the M86 group (or perhaps the NGC4435/8 pair) rather than around M87 itself.

Aside from long ICL streams, many galaxies show tidal features on smaller scales. Perhaps the most obvious is the tidal tail to the north of the interacting pair NGC 4435/8 (D). Originally identified by Malin (1994) in photographic imaging, our imaging traces it to fainter surface brightnesses ($\mu_V>$ 28), where it takes a sudden 90° bend to the west. This kind of tidal "dogleg" is expected during close and slow encounters in a galaxy cluster, where the tidal forces of both the individual galaxies and the cluster itself conspire to create rather complex tidal morphologies (Mihos 2005, in preparation). Other notable features include NGC 4388's tidal plumes to the west and northeast (E), a southern tail in NGC 4425 (F; both noted by Malin 1994) which connects to VCC 987, another tail extending from IC 3349 (G) and passing through VCC 942, and a loop to the east of IC 3475 (H).

At low surface brightness, the giant elliptical M87 shows a very extended and irregular stellar envelope. From photographic images, Weil et al. (1997) and Katsiyannis et al. (1998) show M87's luminous halo extending to $\sim$ 100 kpc scales; on our image it can be traced further out to 175 kpc (I). Here the outer isophotes are not simply the radial extension of M87's inner regular luminosity profile; traced to the northwest, the isophotes become boxier and show irregular loops and shells which may be remnants from earlier stripping from, or cannibalization of, smaller galaxies. The lopsidedness and irregularity of M87's halo is again indicative of a diffuse envelope which is not fully relaxed.

Because of the close proximity of M86, M84, and a number of smaller galaxies, uniquely tracing out any individual halo in that complex of galaxies proves difficult. The isophotes of both M86 and M84 appear fairly regular out to a surface brightness of $\mu_V\sim$ 26.5 (J), as noted by Malin (1994). At fainter surface brightnesses, the isophotes blend together and become quite irregular, and we see a "crown" of diffuse light (at μ_V= 27–28) to the north of the M84/M86 system (K), and a diffuse extension to the south of the pair, blending into the net-

work of galaxies to the south. Whether this extended envelope is truly physical or simply a projection effect remains unclear. Also visible around M86 are several low surface brightness filaments (L1–L3), one to the northeast ($\mu_V\sim$ 25.5), one to the west ($\mu_V\sim$ 26.5), and one to the north ($\mu_V\sim$ 27.5).

We also see a common envelope of light (M) surrounding the complex of galaxies to the south of M86, including NGC 4413, IC 3363, and IC 3349, along with a tidal bridge connecting NGC 4413 and IC 3363, and perhaps extending to NGC 4388 to the east. This envelope has fairly irregular isophotes, arguing it is more than just simply the extended profiles of galaxies overlapping in projection. This group of galaxies may be a physically coherent subgroup within the Virgo cluster.

Finally, Oosterloo & van Gorkom (2005) have recently identified an extended (110x25 kpc) HI cloud streaming from NGC 4388 which they attribute to ram-pressure stripping due to the lack of any stellar counterpart in previous photographic imaging. We also find no extended counterpart on our image down to a surface brightness limit of μ_V=28.5, save for faint streamers close to the main body of NGC 4388 coincident with the extended emission line region noted by Yoshida et al. (2002).

4. DISCUSSION

Our deep imaging of the Virgo cluster has revealed a complex network of extended tidal features, indicative of the ongoing stripping and tidal evolution of galaxies in Virgo. The ICL is not radially symmetric around M87, the nominal central galaxy of Virgo; much of the diffuse light is centered upon the M84/M86 complex. The impact of hierarchical assembly of clusters on the ICL is clear here — rather than ICL growing simply via smooth accretion around a central galaxy, it distribution reflects the substructure inherent in the cluster, as evidenced in cosmologically-motivated N-body simulations of ICL (e.g., Dubinski 1998; Willman et al. 2004, Rudick et al. in preparation). Characterizing the ICL in terms of a simple radial profile will prove misleading in all but the most regular, relaxed clusters.

It is also instructive to compare our map of the ICL in Virgo's core to estimates of the luminosity density derived from studies of planetary nebulae by Feldmeier et al. (2004) and Aguerri et al. (2005). Because IPNe detection depends strongly on the underlying surface brightness, IPNe studies have complicated selection and completeness functions, particularly in fields which cover both bright galaxies and diffuse intracluster space. With this in mind, we will restrict the discussion here to a qualitative comparison, and leave a more quantitative analysis to a future paper.

Both IPNe studies show that the IPNe density is highly variable in the Virgo core; our image confirms this complexity and variation in the underlying ICL. The highest IPNe densities are found in Feldmeier et al.'s "Field 3," which our image shows is completely embedded in M87's diffuse halo. Much of the IPNe detected in this field are likely to be associated with M87 itself; radial velocity measurements of the IPNe in this field agree with this assessment (Arnaboldi et al. 2005). Aguerri et al.'s "SUB" field also shows a relatively high PNe density; aside from containing the luminous ellipticals M84 and M86, this field also partly covers the diffuse envelope surrounding the group of galaxies to the south of M86. The lowest IPNe densities are reported in Aguerri et al.'s "LPC" field, which also corresponds to the lowest luminosity density in our image; indeed, over most of this field, we detect no light above the background.

The qualitative match between the luminosity density traced by IPNe and broadband light argues that IPne are effective tracers of the ICL in galaxy clusters, and vice-versa. Our deep imaging provides a "finding chart" for IPNe searches; followup spectroscopy can then be used to study the kinematics of discrete structures such as tidal tails and diffuse envelopes around galaxies. Our survey of diffuse light in Virgo continues: we have follow-up imaging of additional portions of the Virgo cluster, and subsequent papers will focus on quantitative descriptions of Virgo's ICL, as well as a survey of extremely low surface brightness galaxies in the cluster core.

This work is supported by NSF grants AST-9876143 (JCM), AST-0098435 (HLM), and AST-0302030 (JF), and by Research Corporation Cottrell Scholarships to JCM and HLM.

REFERENCES

Aguerri, J.A.L., Gerhard, O.E., Arnaboldi, M., Napolitano, N.R., Castro-Rodriguez, N., & Freeman, K.C. 2005, AJ, 129, 2585
Arnaboldi, M. et al. 2004, ApJ, 614, L33
Bernstein, G. M., Nichol, R. C., Tyson, J. A., Ulmer, M. P., & Wittman, D. 1995, AJ, 110, 1507
Binggeli, B.,Sandage, A., & Tammann, G.A. 1987, AJ, 94, 251
Binggeli, B., Popescu, C. C., & Tammann, G. A. 1993, A&AS, 98, 275
Dubinski, J. 1998, ApJ, 502, 141
Durrell, P., Ciardullo, R., Feldmeier, J. J., Jacoby, G. H., & Sigurdsson, S. 2002, ApJ, 570, 119
Feldmeier, J. J., Ciardullo, R., Jacoby, G. H., & Durrell, P.R. 2004, ApJ, 615, 196
Feldmeier, J.J., Mihos, J.C., Morrison, H.L., Rodney, S.A., & Harding, P.H. 2002, ApJ, 575, 779
Feldmeier, J.J., Mihos, J.C., Morrison, H.L., Harding, P.H., Kaib, N., & Dubinski, J. 2004, ApJ, 609, 617
Ferguson, H. C., Tanvir, N. R., & von Hippel, T. 1998, Nature, 391, 461
Gerhard, O., Arnaboldi, M., Freeman, K.C., Kashikawa, N., Okamura, S., & Yasuda, N. 2005, ApJ, 621, L93
Katsiyannis, A. C., Kemp, S. N., Berry, D. S., & Meaburn, J. 1998, A&AS, 132, 387
Malin, D. 1994, IAU Symp. 161: Astronomy from Wide-Field Imaging, 161, 567
Murante, G., et al. 2004, ApJ, 607, L83
Oosterloo, T., & van Gorkom, J. 2005, A&A, 437, 190
Rubin, V. C., Waterman, A. H., & Kenney, J. D. P. 1999, AJ, 118, 236
Sommer-Larsen, J., Romeo, A. D., & Portinari, L. 2005, MNRAS, 357, 478
Uson, J. M., Boughn, S. P., & Kuhn, J. R. 1991, ApJ, 369, 46
Vílchez-Gómez, R. 1999, ASP Conf. Ser. 170: The Low Surface Brightness Universe, 349
Weil, M.L., Bland-Hawthorn, J., & Malin, D.F. 1997, ApJ, 490, 664
Willman, B., Governato, F., Wadsley, J., & Quinn, T. 2004, MNRAS, 355, 159
Yoshida, M. et al. 2002, ApJ, 567, 118